Modeling of Resonant TE Waves for Electron Cloud Density Measurements in CesrTA

Danielle Duggins

CLASSE 2012 REU

Abstract

Maximizing the current and stability of the beam is an important goal in high-energy accelerators. Low-energy electron clouds can be produced from photoemission caused by synchrotron radiation, ionization of residual gas in beam-pipe, and secondary electrons. In lepton accelerators like CesrTA, low-energy electron clouds form primarily from synchrotron radiation of a positron beam and cause destabilization and lower the maximum possible total beam current [1]. The resonant TE wave technique is used to measure the electron cloud density in an accelerator. This method uses microwaves to resonantly excite standing waves the beam-pipe. The presence of an electron cloud within this standing wave will shift its resonant frequency slightly and the effect can be observed with a spectrum analyzer. In some beam-pipe geometries, the standing waves can be highly localized. For example, the geometries of some sections of CesrTA have lower cutoff frequencies than the surrounding beam-pipe. This can confine some of the resonances – and their sensitivity to the electron cloud - to those short sections. This paper contains simulation and experimental results to show how resonant TE wave measurements can be localized.

1 Introduction

Methods for measurement of Electron Cloud Densities being pursued at CesrTA include measuring beam responses to electron cloud (i.e. measuring the tune shift of the beam), collection of electrons and current measurment (e.g. RFA & Shielded Pickup), and the TE Wave Method. Measuring electron cloud through the tune shift will measure the EC density in the entire accelerator, RFAs and shielded pickup measurements only measure electrons leaving the chamber at points along the pipe, while the TE wave technique measures the electron cloud density over a finite length. The TE wave technique uses existing Beam Position Monitor (BPM) buttons to couple microwaves into the beam-pipe. Resonances can then be produced in the beampipe and the density of the electron cloud can be measured by observing the effect of the resonant frequency shift in the presence of an electron cloud density (ECD).

A new beam-pipe assembly was installed summer of 2012. The assembly contains four separate sections for testing the effectiveness of electron cloud mitigation techniques. There are two sections of round bare aluminum chamber, one smooth, the other with grooves on the top and bottom of the inner surface. The other two sections have the same geometry but the aluminum is coated with Titanium Nitride (TiN). The grooved sections of beam-pipe have lower cutoff frequencies than the smooth beam-pipe, causing reflections at each end of the section. This allows TE wave technique to measure the EC density inside a specific volume over a finite length of the pipe by creating standing waves in that section.

Resonances at other sections of the accelerator have been studied through experiment and simulation and it has been confirmed that the resonant frequency shifts in the presence of an electron cloud.

2 Grooved Beam-Pipe

Two beam-pipe chamber geometries were installed in the new beam-pipe assembly. The first is a simple circular waveguide (smooth) and the second is circular with grooved sections at the top and bottom of the waveguide. The grooved pipe geometry was installed in the accelerator for attenuation of the ECD.

The grooved chambers have been designed to work in the presence of the external dipole field. This field causes electrons in the cloud to tend to move vertically in the pipe. Electrons hitting the top and bottom of the pipe at the grooves are no longer normal to surface of the pipe and as they "bounce around" within the grooves, they will lose their energy to the grooves and are far less likely to produce secondary electrons.

In the new assembly, grooved and smooth pipe sections alternate. It was observed through experi-

ment that it was possible to trap TE waves within the grooved pipe section when excited at the correct frequencies. This lead to speculation that the grooved pipe chamber had a lower cutoff frequency than the smooth chamber. When frequencies between the two cutoffs were used, standing waves in the grooved chamber were formed. This idea is confirmed by simulations addressed in this paper.

3 Vorpal Simulations

For simulation, a program called VORPAL was used. VORPAL solves Maxwell's equations numerically and handles both particles and fields.[2]

In order to implement the grooved-pipe geometry the Fourier series for a triangle wave was used and parameters were based on blueprints of the actual geometry of the beam-pipe.

$$f(x) = \frac{8}{\pi^2} \sum_{n=odd}^{\infty} \frac{(-1)^{(n-1)/2}}{n^2} \sin\left(\frac{n\pi x}{L}\right) \qquad (1)$$

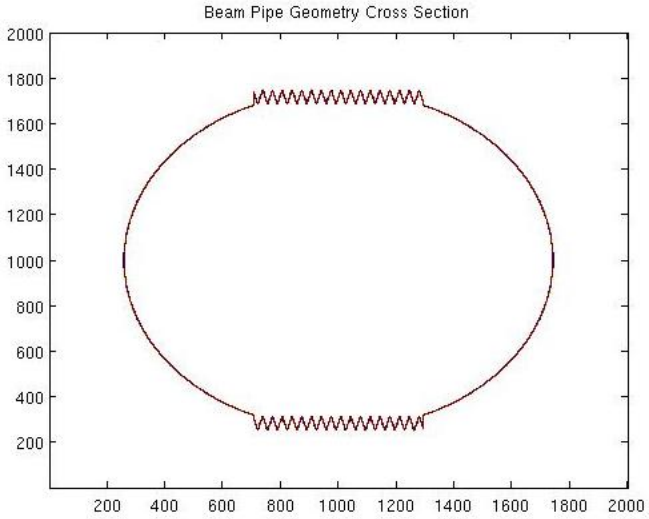

Figure 1: Cross sectional view of the beam-pipe with grooves from VORPAL

A python function was written and called upon by VORPAL to create this geometry. A conducting surface marks the transverse boundary. At both ends of the computational domain, a perfectly matched layer (PML) is used. The PML, invented by Bérenger, is absorptive, preventing reflections, and causing exponential decay of the propagating wave [3]. Bérenger's PML uses electrically and magnetically conductive surfaces to attenuate both the electric and magnetic field in the PML. Magnetic current is non-physical, but serves to absorb the magnetic field. Adding a term to Maxwell's Equations is how this is accomplished [3]:

$$\epsilon_0 \frac{\partial E}{\partial t} + \sigma E = \nabla \times H$$

$$\mu_0 \frac{\partial H}{\partial t} + \sigma^* H = -\nabla \times E$$

VORPAL solves these equations at the PML, creating exponential decay and minimizing reflections.

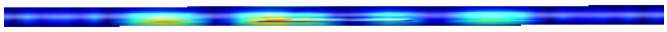

Figure 2: view of TE wave propagation and absorption at PMLs at either end from VORPAL

3.1 Cutoff Frequencies

First, a smooth-pipe geometry was implemented in VORPAL to observe the cutoff frequency and then a grooved-pipe geometry was implemented. A current source at a location just left of center was used to propagate a TE wave through the pipe. Frequency scans were performed over a range of frequencies near the expected cutoff. Voltage measurements were taken along the length of the pipe as the wave was being generated and a plot of the measurements was made in MATLAB, showing the electric field vs. position along the length of the beam-pipe. The frequency at which the electric field propagated through the pipe rather than decayed from the drive point was the cutoff frequency for that geometry. As expected, the grooved-pipe had a lower cutoff frequency.

An example of the electric field plot is shown in Figure 3:

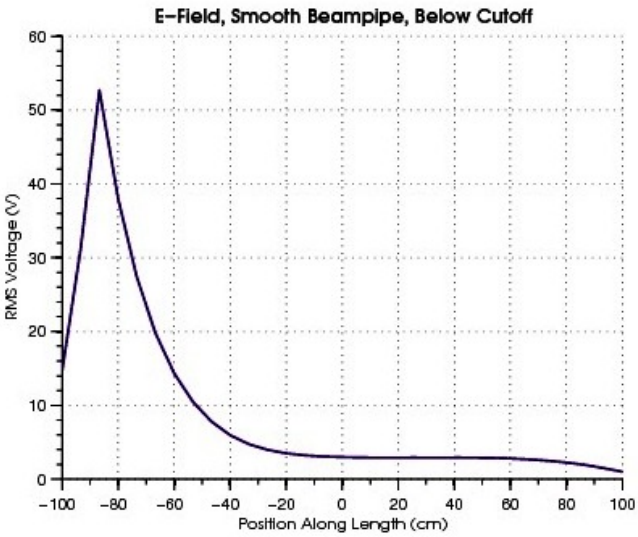

Figure 3: MATLAB plot of voltage data taken from VORPAL

The cutoff frequency of the smooth-only geometry was found to be $f_c = 1.974GHz$, which agrees

with the theory for a circular waveguide. The cutoff frequency of the grooved-only pipe was found to be $f_c = 1.875GHz$.

3.2 Frequency Scans

A chamber was then created using a python function to make a geometry in VORPAL that would consist of three sections of pipe, two smooth and a grooved section in the center.

Figure 4: smooth-grooved-smooth beam-pipe lengthwise view from VORPAL simulation

TE waves were excited in the grooved section of the beam-pipe at frequencies ranging from below the cutoff of both geometries to above the cutoff of both. Similar scans were done for geometries with half the length of grooves, quarter length of grooves, eighth length of grooves, with and without an electron cloud. At locations where the existence of resonances looked probable, finer scans of frequencies were performed.

3.3 Determination of Resonances

The existence of standing waves in the grooved section of pipe was determined using amplitude, shape and phase of the electric field along the pipe. Plotting the RMS voltage along the length of pipe shows the shape and amplitude of the electric field. At certain frequencies, the amplitude of the electric field was much greater and the shape of the electric field was that of some number of half wave length standing waves. This was true for the $n = 1$ and $n = 2$ resonances. At $n = 3$, the standing wave propagated out into the smooth pipe and the amplitude of the electric-field was much lower, indicating that the frequency for $n = 3$ is above the cutoff of both chambers and would not be useful in isolated measurements in the grooved section for EC density.

The voltage data at each location contains information about the wave at that point. We can say that:

$$V_1 = A_1 \sin(\omega t + \phi_1)$$

First we take the rms value, and we can say:

$$A_1 = V_{rms}\sqrt{2}$$

Dividing V by A_1 we get:

$$\sin(\omega t + \phi_1)$$

We can then use a trig identity and inverse sin to isolate $(\phi_1 - \phi_2)$

$$\sin(\omega t + \phi_1) - \sin(\omega t + \phi_2)$$

$$= 2\sin(\frac{\phi_1 - \phi_2}{2})\cos(\omega t + \frac{\phi_1 + \phi_2}{2})$$

Taking the inverse sine gives us numbers proportional to the phase shift along the length as compared to the drive point. If we normalize, we can get minima at $0rad$ and maximas at πrad. The phase difference was taken using the voltage at the drive point and comparing that to the voltage at the rest of the length of pipe. The average phase difference along the length of the grooves is then calculated. For $n = 1$, the resonances are determined at minima of the average phase difference. Using that data and the amplitude, it was determined that there was a resonance occurring in the grooved pipe for one-half wavelength.

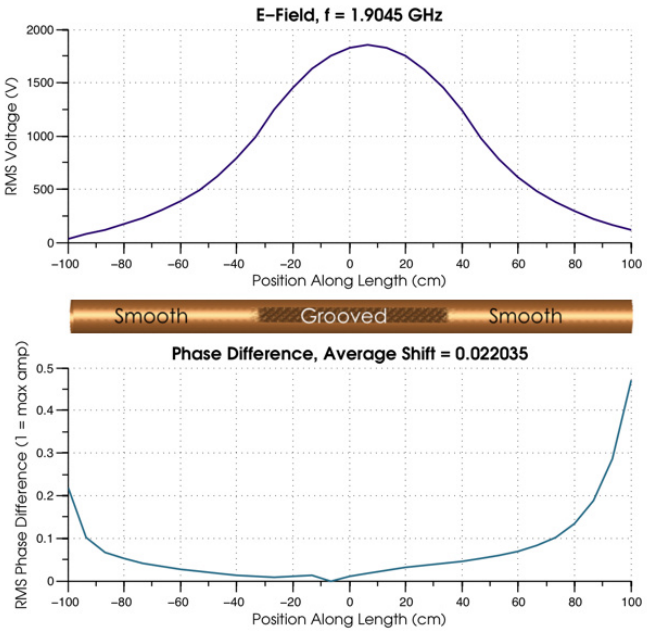

Figure 5: $n = 1$ mode

For $n = 2$ resonances are seen when one of the half wave length has a phase difference close to zero

and the other half wavelength has a phase difference close to πrad. Having a phase difference close to π indicates that that half wavelength is exactly out of phase with the other side. The average phase shift is computed for the left and right sides of the chamber separately. The n=2 resonance was also determined to exist within the grooved pipe.

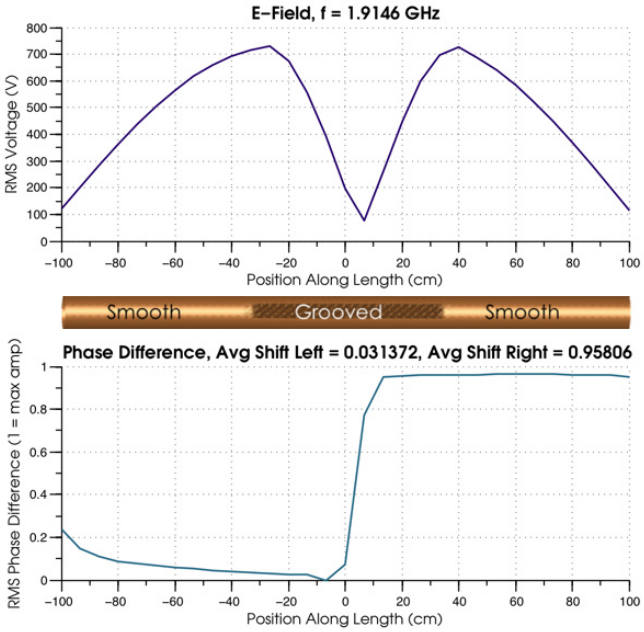

Figure 6: $n = 2$ mode

3.4 Shortening Grooved Length

In previous experiments an evanescent mode was observed in a short (2cm long) flange in the beampipe [4]. It was hypothesized that in the limit that the grooved pipe became short enough, an evanescent-like mode would be observable. This would lead to an exponential decrease in amplitude along the length in both directions. This mode is of interest as another way of providing a localized measurement of EC density. Thus, more frequency scans were performed for the same total length of pipe, but with half, quarter and eighth the length of the grooves. The $n = 1$ and $n = 2$ resonances were still observed, but with the resonant frequencies shifted up, as shown on the graphs. The upward shift of the resonant frequencies is expected due to the behavior of standing waves. For standing waves with perfect reflections in a waveguide,

$$f^2 = f_c^2 + (\frac{nc}{2L})^2 \tag{2}$$

Since the wavelength will decrease as the length decrease, we expect in our system for the resonant frequencies to increase, though without perfect reflections, the equation doesn't hold. Results are in figures 7, 8, and 9.

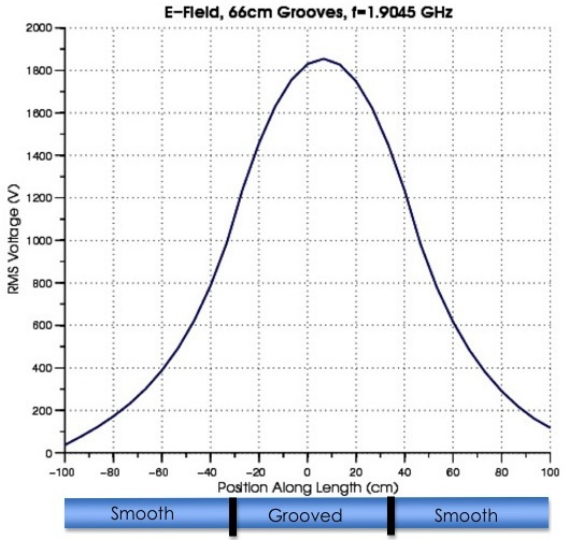

Figure 7: 66cm long grooves

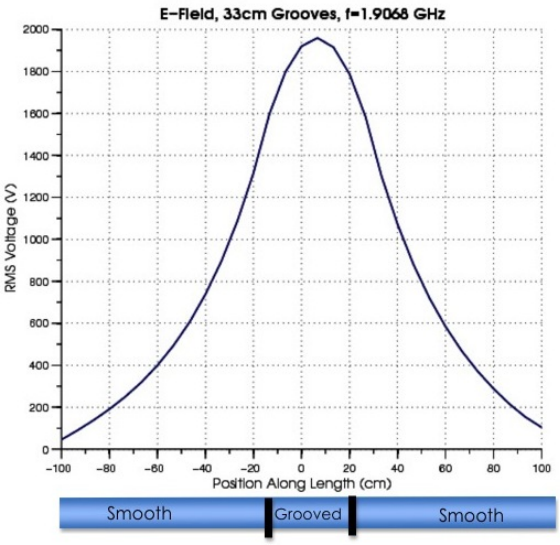

Figure 8: 33cm long grooves

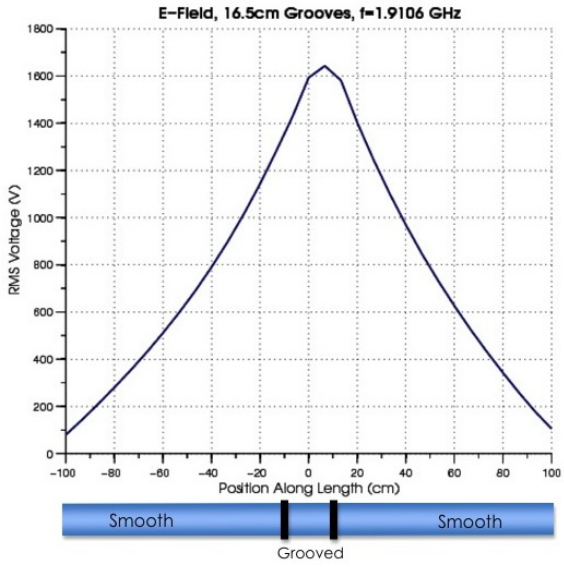

Figure 9: 16.5cm long grooves

3.5 Effects of Electron Cloud

The shift in resonance for a cavity due to EC density is:

$$\frac{\Delta\omega_n}{\omega} = \frac{e^2}{2\epsilon_0 m_e \omega^2} \frac{\int_V n_e E_0^2 dV}{\int_V E_0^2 dV} \quad (3)$$

Simulations were then run with two different densities of electron cloud. The resonant frequencies were determined using the same method as above. The resonant frequencies for $n = 1$ and $n = 2$ were studied and seen to be shifted up. According to equation 3 and using the density of $n_e = 1e14$ and for $\frac{\omega}{2\pi} = 2GHz$. The frequency shift should be:

$$\frac{\Delta\omega}{2\pi} \approx 2MHz$$

Table 1 agrees well with the theory since the frequency shifts are in the range of 2 MHz.

Frequencies of First Resonance (GHz)			
Groove Length	E-Cloud Density		
	No e^-	$1e14$	$2e14$
Whole	1.9045	1.907	1.910
Half	1.9068	1.910	1.912
Quarter	1.9107	1.913	1.916

Table 1: $n = 1$ mode - varying groove length and e-cloud density

The next table of data, Table 2, for the $n = 2$ mode does not agree quite as well with the equation since each frequency shift is only about 1 MHz.

Frequencies of Second Resonance (GHz)			
Groove Length	E-Cloud Density		
	No e^-	$1e14$	$2e14$
Whole	1.9146	1.9155	1.917
Half	1.9167	1.9175	1.918
Quarter	1.9177	1.9185	1.919

Table 2: $n = 2$ mode - varying groove length and e-cloud density

4 Experimental: Bead Pull Method

The effect of dielectrics on a cavity is similar to that of the EC density in terms of frequency shift. The equation is:

$$\frac{\Delta\omega}{\omega} = \frac{\int_V (1-\varepsilon_r) E_0^2 dV}{2\int_V E_0^2 dV}$$

By positioning a small dielectric inside the beam pipe at locations along the length, the frequency shift can be observed and is proportional to the electric field strength squared at that point. This technique is used to "map" the electric field squared vs. the position of the bead in the beam-pipe and observe resonances confined to particular sections of the chamber. During a down in July at CesrTA, a new beam-pipe assembly was installed in L3. Before the pipe was installed, measurements were taken using the TE wave bead pull technique. Microwaves were excited and responses recorded at the three BPMs on the assembly at various frequencies. Resonances were observed occurring locally in the grooved pipe. Figure 10 shows a diagram of the assembly that was measured and Figure 11 shows a basic diagram of the beadpull method.

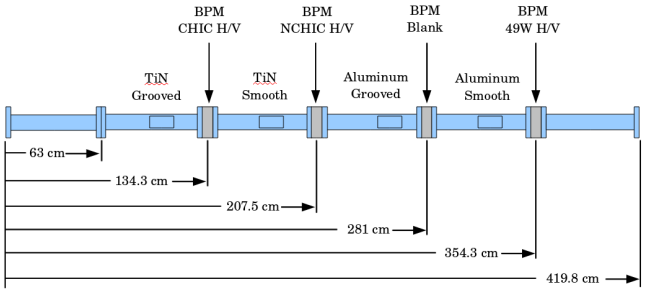

Figure 10: Beadpull Bench Diagram

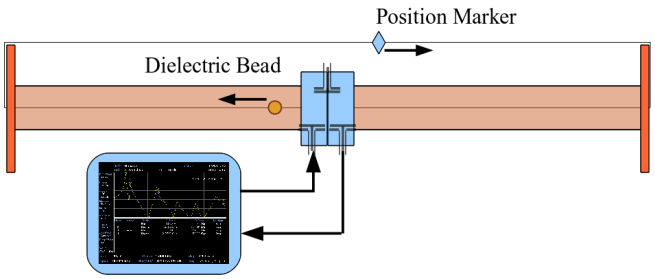

Figure 11: Beadpull Method Diagram

Some of the measurements made using the bead pull method are shown in Figures 12 - 16 below. An arrow in each figure indicates the position of the drive point of the electric field. Resonant modes are shown in each of the grooved chambers. Consistent with the simulation data, the $n = 3$ mode propagated out into the smooth pipe, confirming the resonant frequency is above the cutoff frequency of both the smooth and grooved chambers. This results in a smaller electric field strength, as seen in Figure 16.

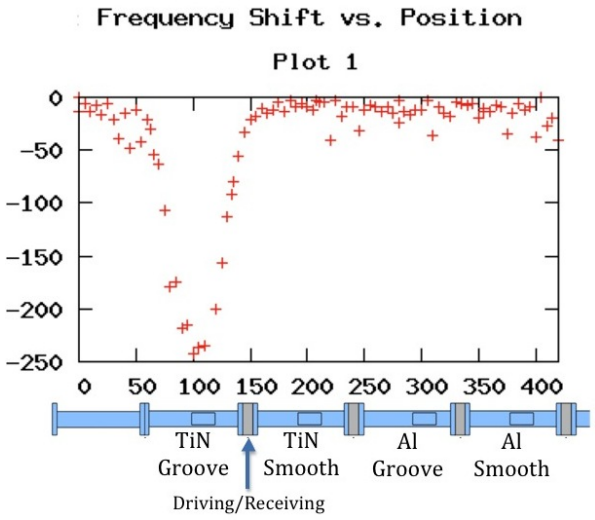

Figure 12: the $n = 1$ mode within the first chamber of grooved titanium nitride

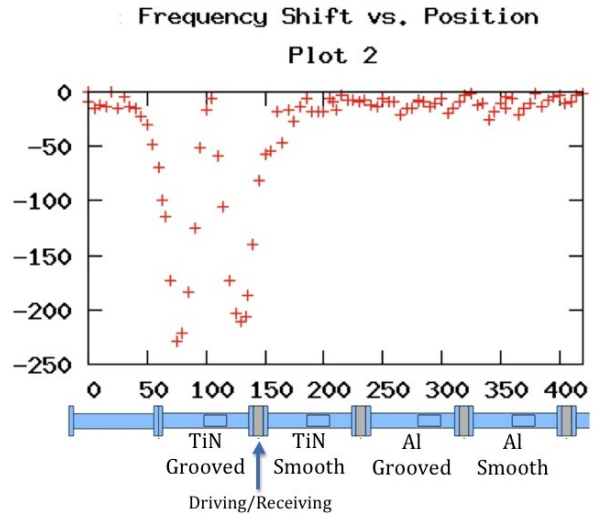

Figure 13: the $n = 2$ mode within the first chamber of grooved titanium nitride

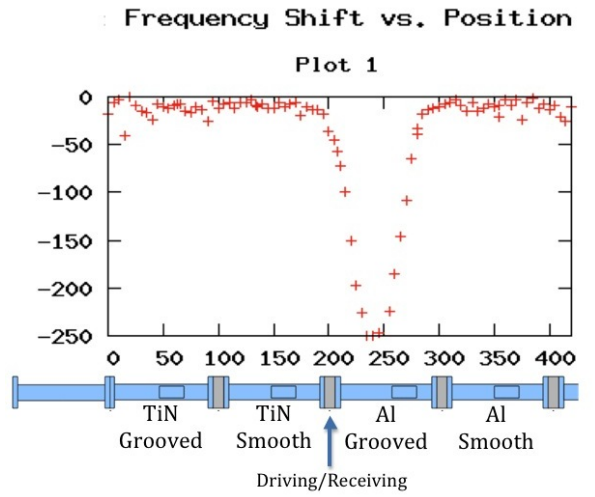

Figure 14: the $n = 1$ mode within the third chamber of grooved aluminum

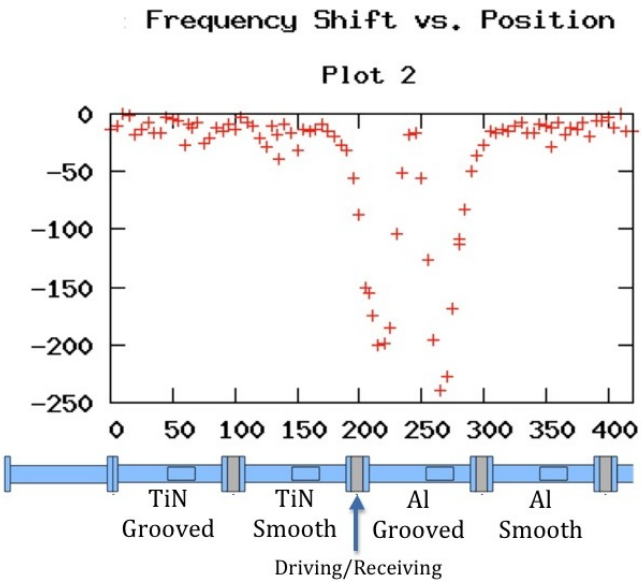

Figure 15: the $n = 2$ mode within the third chamber of grooved aluminum

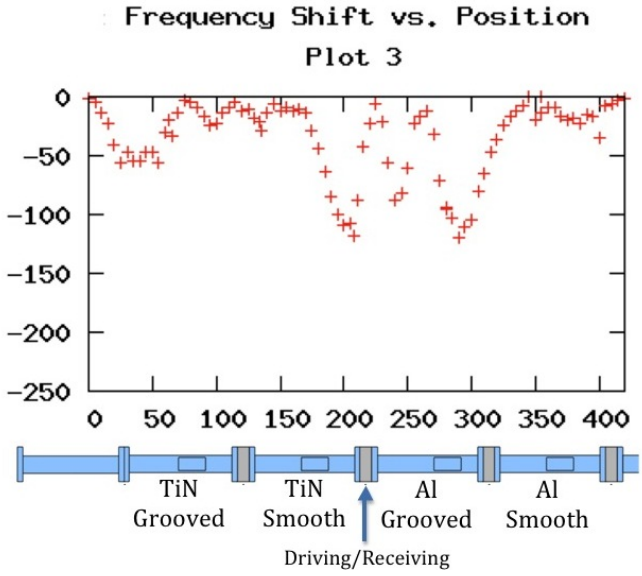

Figure 16: the $n = 3$ mode within the third chamber of grooved aluminum

5 Future Work

Now that the standing waves in L3 chamber are better understood, data collection with beam can be improved. For example, the frequencies that produce localized resonances should be used so that independent EC density measurements can be made of the different sections of the L3 chamber.

In most cases, it is not possible to perform bead-pull measurements on beam-pipe as when it has already been installed in the accelerator. A new measurement technique for the beam-pipe already installed in the accelerator might be developed. One candidate is something of a deformation measure-

ment. If the beam-pipe could be deformed a certain amount, a frequency shift could be observed in the electric field and a similar mapping to the bead pull technique of the electric field could be accomplished. This technique is still being developed and other measurement techniques must be considered. The evanescent mode of the chamber has not been fully investigated as a useful measurement and could use further simulation.

The experimental bead pull method was consistent with the simulation data regarding resonances of n=1 and n=2 occurring in the grooved pipe. This is consistent with theory and could be developed into a useful technique for measuring EC density that is non-invasive, localized and cheap. This would lead to determination of which implementations in the accelerator attenuate the creation of electron cloud and eventually raising the maximum current and stability of the beam.

References

[1] S. De Santis, J.M. Byrd, F. Caspers, A. Krasnykh, T. Kroyer, M.T.F. Pivi, and K.G. Sonnad. "Measurement of Electron Clouds in Large Accelerators by Microwave Dispersion." Phys. Rev. Lett. PRL 100, 094801 (2008).

[2] C. Nieter and J. R. Cary. "VORPAL: a versatile plasma simulation code." J. Comp. Phys. 196, 448 (2004)

[3] A. Bondeson, T. Rylander, and P. Ingelstr'om. *Computational Electromagnetics* New York, Springer, Chapter 5.

[4] J.P. Sikora, M.G. Billing, M.A. Palmer, K.G. Sonnad, B.T. Carlson, K.C. Hammond, and S. De Santis. "Resonant TE Wave Measurements of Electron Cloud Density at CesrTA." *Proceedings of IPAC2011, San Sebastián, Spain* (2011)

[5] S. De Santis, J. Sikora, and D. Alesini. "Analysis of Resonant TE Wave Modulation Signals For Electron Cloud Measurements."

[6] K. Yee. "Numerical solution of initial boundary value problems involving Maxwell's equations in isotropic media." IEEE Transactions on Antennas and Propagation, AP-14, 302 (1966)

[7] K. Sonnad, M. Furman, S. Veitzer, P. Stoltz, and J. Cary. "Simulation and analysis of microwave transmission through an electron cloud: a comparison of results." *Proceedings of PAC07, Albuquerque, NM* (2007)

[8] J.P. Sikora, M.G. Billing, D.L. Rubin, R.M. Schwartz, D. Alesini, B.T. Carlson, K.C. Hammond, and S. De Santis. "Using TE Wave Resonances For The Measurement of Electron Cloud Density."